Chair for Security in Information Technology
School of Computation, Information and Technology
Technical University of Munich

Towards Efficient Helper Data Algorithms for Multi-Bit PUF Quantization

Marius Drechsler

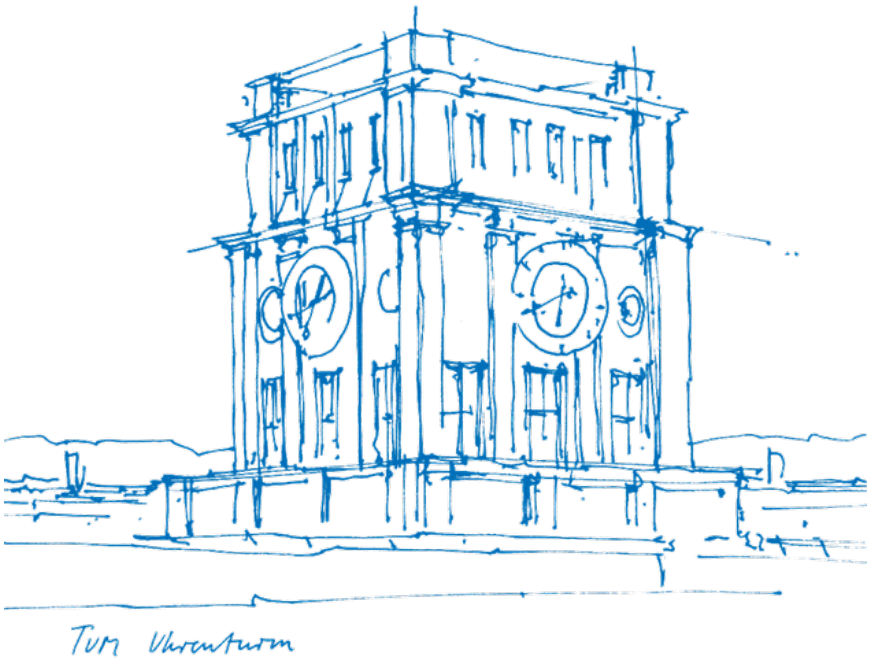

Chair for Security in Information Technology
School of Computation, Information and Technology
Technical University of Munich

Towards Efficient Helper Data Algorithms for Multi-Bit PUF Quantization

Marius Drechsler

Thesis for the attainment of the academic degree

Bachelor of Science (B.Sc.)

at the School of Computation, Information and Technology of the Technical University of Munich.

Examiner:
Prof. Dr. Georg Sigl

Supervisor:
M.Sc. Jonas Ruchti

Submitted:
Munich, 22.07.2024

Contents

1 Introduction

These are the introducing words

1.1 Notation

To ensure a consistent notation of functions and ideas, we will now introduce some required conventions

Random distributed variables will be notated with a capital letter, i.e. X, its realization will be the corresponding lower case letter, x.

Vectors will be written in bold test: $\boldsymbol{k}$ represents a vector of quantized symbols.

We will call a quantized symbol k. k consists of all possible binary symbols, i.e. $0, 01, 110$.

A quantizer will be defined as a function $\mathcal{Q}(x, \boldsymbol{a})$ that returns a quantized symbol k. We also define the following special quantizers for metric based HDAs: A quantizer used during the enrollment phase is defined by a calligraphic $\mathcal{E}$. For the reconstruction phase, a quantizer will be defined by a calligraphic $\mathcal{R}$

Figure 1 shows the curve of a 2-bit quantizer that receives $\tilde{x}$ as input. In the case, that the value of $\tilde{x}$ equals one of the four bounds, the quantized value is chosen randomly from the relevant bins.

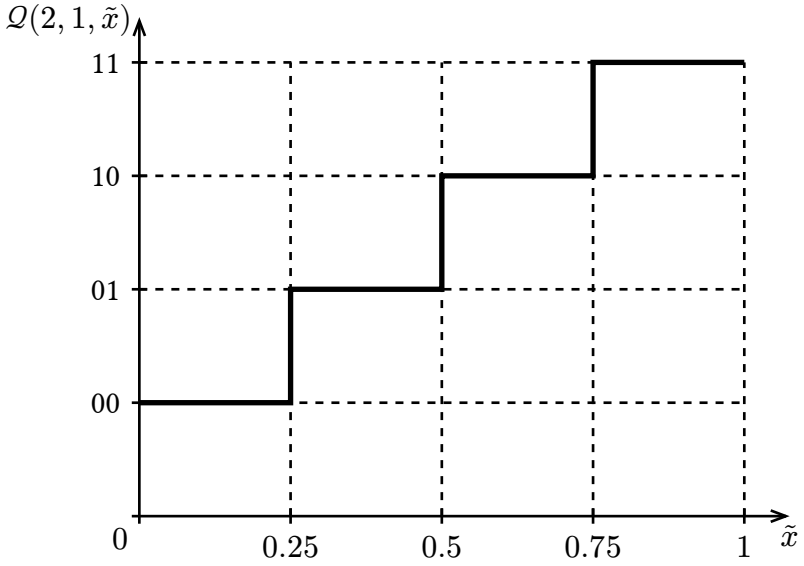

Figure 1: Example quantizer function

For the S-Metric Helper Data Method, we introduce a function

$$\mathcal{Q}(S, M), \tag{1}$$

where S determines the number of metrics and M the bit width of the symbols. The corresponding metric is defined through the lower case s, the bit symbol through the lower case m.

1.1.1 Tilde-Domain

AS also described in [1], we will use a CDF to transform the real PUF values into the Tilde-Domain This transformation can be performed using the function $\xi = \tilde{x}$. The key property of this transformation is the resulting uniform distribution of x.

Considering a normal distribution, the CDF is defined as

$$\xi\left(\frac{x-\mu}{\sigma}\right) = \frac{1}{2}\left[1 + erf\left(\frac{x-\mu}{\sigma\sqrt{2}}\right)\right] \tag{2}$$

ECDF

The eCDF is constructed through sorting the empirical measurements of a distribution [2]. Although less accurate, this method allows a more simple and less computationally complex way to transform real valued measurements into the Tilde-Domain. We will mainly use the eCDF in Section 2 because of the difficulty of finding an analytical description for the CDF of a Gaussian-Mixture.

2 S-Metric Helper Data Method

A metric based helper data algorithm (HDA) generates helper data at PUF enrollment to provide more reliable results at the reconstruction stage. Each of these metrics correspond to a quantizer with different bounds to lower the risk of bit or symbol errors during reconstruction. For this kind of HDA, the generated metric is used as helper data and thus does not have to be kept secret.

2.1 Background

Before we turn to a concrete realization of the S-Metric method, let's take a look at its predecessor, the Two-Metric Helper Data Method.

2.1.1 Two-Metric Helper Data Method

The most simple form of a metric-based HDA is the Two-Metric Helper Data Method, since the quantization only yields symbols of 1-bit width and uses the least amount of metrics possible if we want to use more than one metric.

Figure 2 and Figure 3 illustrate an example enrollment and reconstruction process. We would consider the marked point the value of the initial measurement and the marked range our margin of error. If we now were to use the original quantizer shown in Figure 2 during both the enrollment and the reconstruction phases, we would risk a bit error, because the margin of error overlaps with the lower quantization bound $-a$, which we can call a point of uncertainty. But since we generated helper data during enrollment as depicted in Figure 4, we can make use of a different quantizer $\mathcal{R}(1, 2, x)$ whose boundaries do not overlap with the error margin.

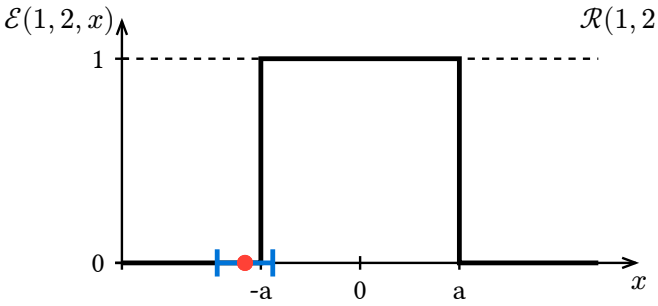

Figure 2: Example enrollment

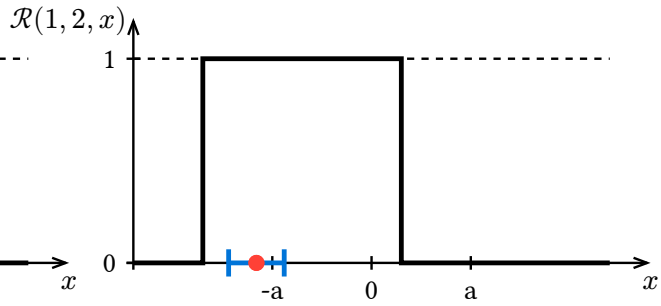

Figure 3: Example reconstruction

Publications [3] and [4] find all the relevant bounds for the enrollment and reconstruction phases under the assumption that the PUF readout (our input value x) is zero-mean Gaussian distributed. Because the parameters for symbol width and number of metrics always stays the same, we can – without loss of generality – assume the standard deviation as $\sigma = 1$ and calculate the bounds for 8 equi-probable areas for this distribution. This is done by finding two bounds a and b such, that

$$\int_a^b f_{X(x)} dx = \frac{1}{8} \tag{3}$$

This operation yields 9 bounds defining these areas $-\infty$, $-T1$, $-a$, $-T2$, 0, $T2$, a, $T1$ and $+\infty$. During the enrollment phase, we will use $\pm a$ as our quantizing bounds, returning 0 if the The corresponding metric is chosen based on the following conditions:

$$M = \begin{cases} M1, x < -a \vee 0 < x < a \\ M2, -a < x \vee 1 < a < x \end{cases}. \tag{4}$$

Figure 4 shows the curve of a quantizer $\mathcal{Q}$ that would be used during the Two-Metric enrollment phase. At this point we will still assume that our input value x is zero-mean Gaussian distributed.

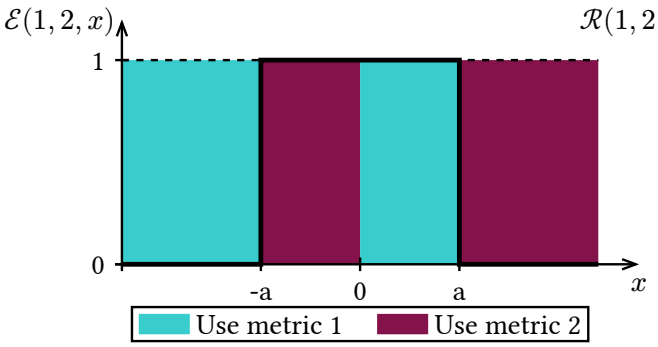

Figure 4: Two-Metric enrollment

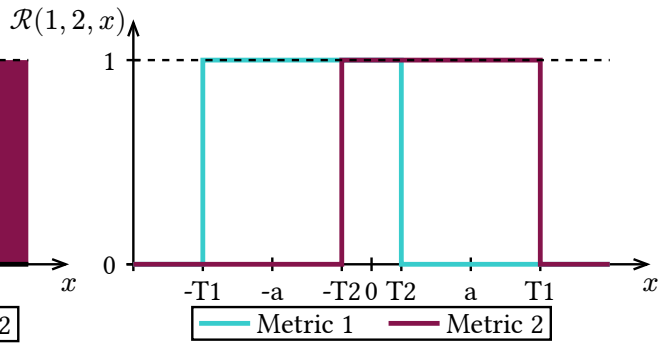

Figure 5: Two-Metric reconstruction

As previously described, each of these metrics correspond to a different quantizer. Now, we can use the generated helper data in the reconstruction phase and define a reconstructed bit based on the chosen metric as follows:

$$M1 : k = \begin{cases} 0, x < T1 \vee T2 < x \\ 1, -T1 < x < T2 \end{cases}, \qquad M2 : k = \begin{cases} 0, x < -T2 \vee T1 < x \\ 1, -T2 < x < T1 \end{cases}.$$

Figure 5 illustrates the basic idea behind the Two-Metric method. Using the helper data, we will move the bounds of the original quantizer (Figure 2) one octile to each side, yielding two new quantizers. The advantage of this method comes from moving the point of uncertainty away from our readout position.

2.1.2 S-Metric Helper Data Method (SMHD)

Going on, the Two-Metric Helper Data Method can be generalized as shown in [1]. This generalization allows for higher-order bit quantization and the use of more than two metrics.

A key difference to the Two-Metric approach is the alignment of quantization areas. Methods described in [3] and [4] use two bounds for 1-bit quantization, namely $\pm a$. Contrary, the method introduced by Fischer in [1] would look more like a sign-based quantizer if the configuration $\mathcal{Q}(2,1)$ is used, using only one quantization bound at $x = 0$. Figure 6 and Figure 7 illustrate this difference, .

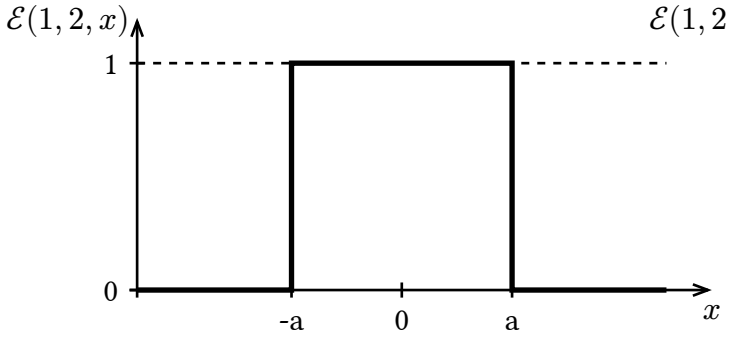

Figure 6: Two-Metric enrollment

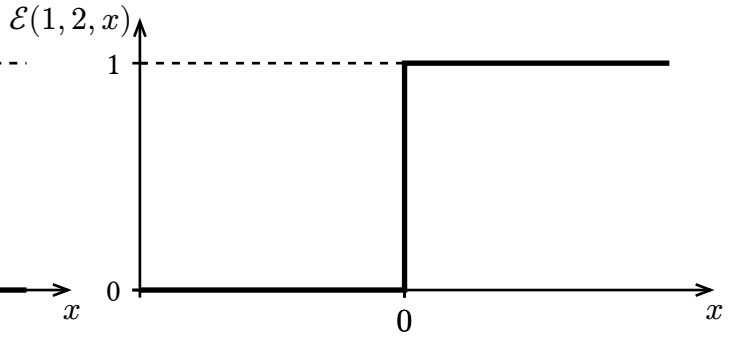

Figure 7: S-Metric enrollment with 1-bit configuration

The generalization consists of two components:

- **Higher-order bit quantization**
  We can introduce more steps to our quantizer and use them to extract more than one bit out of our PUF readout.
- **More than two metrics**
  Instead of splitting each quantizer into only two equi-probable parts, we can increase the number of metrics at the cost of generating more helper data to increase reliability.

2.2 Realization

We will now propose a specific realization of the S-Metric Helper Data Method.
This allows us to use equi-distant bounds for the quantizer instead of equi-probable ones.

From now on we will use the following syntax for quantizers that use the S-Metric Helper Data Method:

$$\mathcal{Q}(S, M, \tilde{x}), \tag{6}$$

where S defines the number of metrics, M the number of bits and $\tilde{x}$ a Tilde-Domain transformed PUF measurement.

2.2.1 Enrollment

To enroll our PUF key, we will first need to define the quantizer for higher order bit quantization and helper data generation. Because our transformed PUF readout $\tilde{x}$ can be interpreted as a realization of a uniformly distributed variable $\tilde{X}$, we can define the width Δ of our quantizer bins as follows:

$$\Delta = \frac{1}{2^M}. \tag{7}$$

For example, if we were to extract a symbol with the width of 2 bits from our PUF readout, we would need to evenly space $2^2 = 4$ bins. Using equation Equation 7, the step size for a 2-bit quantizer would result to:

$$\Delta' = \frac{1}{2^M}\bigg|_{M=2} = \frac{1}{4}. \tag{8}$$

Figure 8 shows a plot of the resulting quantizer function that would yield symbols with two bits for one measurement $\tilde{x}$.

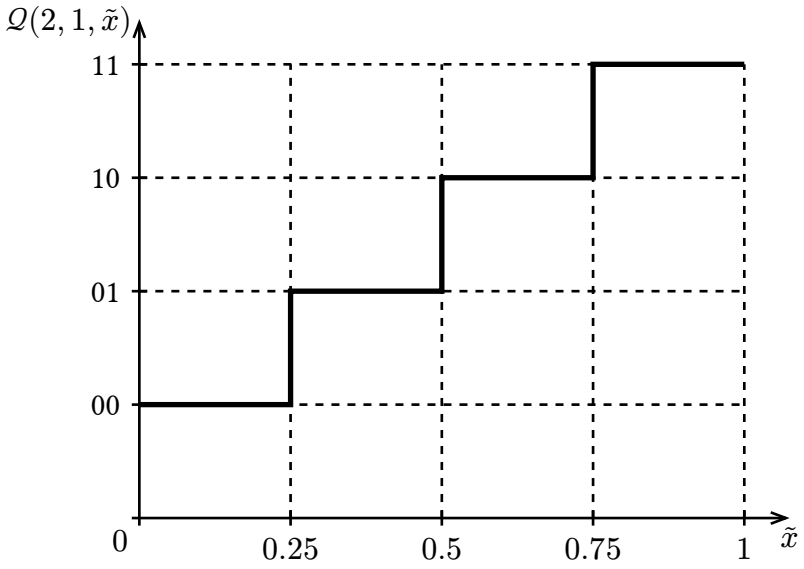

Figure 8: 2-bit quantizer

Right now, this quantizer wouldn't help us generating any helper data. To achieve that, we will need to divide a symbol step – one, that returns the corresponding quantized symbol - into multiple substeps. Using S, we can define the step size Δ_S as the division of Δ by S:

$$\Delta_S = \frac{\Delta}{S} = \frac{\frac{1}{2^M}}{S} = \frac{1}{2^M \cdot S} \tag{9}$$

We can now redefine our previously defined quantizer function to not only return the quantized symbol, but a tuple consisting of the quantized symbol and the metric ascertained that we will save as helper data for later.

Going on in our example, we could choose the amount of our metrics to be 2. According to Equation 9, we would then half our step size:

$$\Delta'_S = \frac{\Delta'}{S}\bigg|_{S=2} = \frac{1}{4 \cdot 2} = \frac{1}{8} \tag{10}$$

This means, we can update our quantizer function with the new step size $\Delta'_S = \frac{1}{8}$ and redefining its output as a tuple consisting of bit value and helper data.

We can visualize the quantizer that we will use during the enrollment phase of a 2-bit 2-metric configuration as depicted in Figure 9.

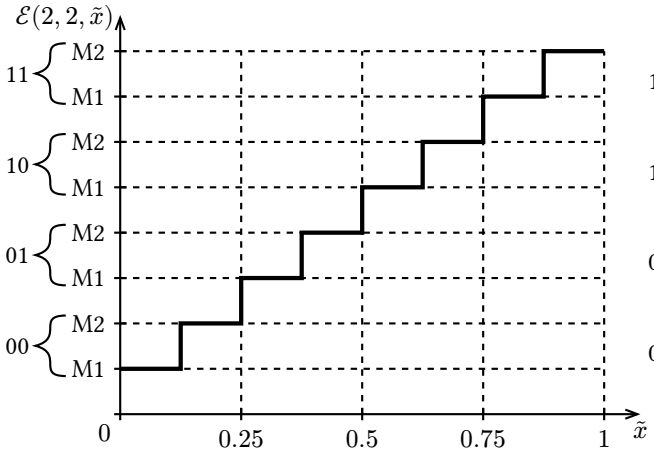

Figure 9: 2-bit 2-metric enrollment

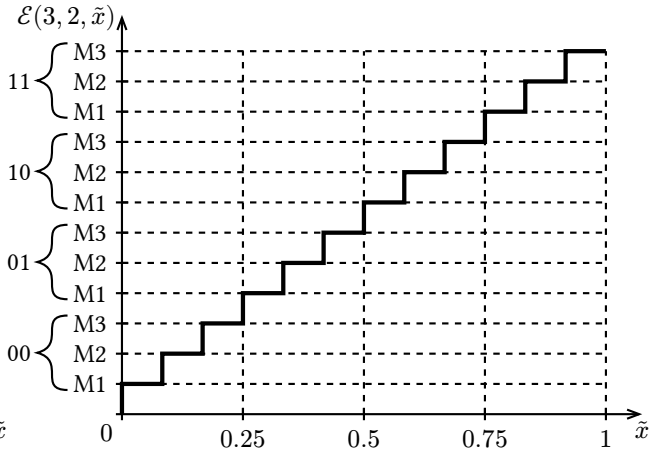

Figure 10: 2-bit 3-metric enrollment

To better demonstrate the generalization to S-metrics, Figure 10 shows a 2-bit quantizer that generates helper data based on three metrics instead of two. In that sense, increasing the number of metrics will increase the number of sub-steps for each symbol.

We can now perform the enrollment of a full PUF readout. Each measurement will be quantized with out quantizer $\mathcal{E}$, returning a tuple consisting of the quantized symbol and helper data.

$$K_i = \mathcal{E}(s, m, \tilde{x_i}) = (k, h)_i \quad . \tag{11}$$

Performing the operation of Equation 11 for our whole set of measurements will yield a vector of tuples $\boldsymbol{K}$.

2.2.2 Reconstruction

We already demonstrated the basic principle of the reconstruction phase in section Section 2.1.1, which showed the advantage of using more than one quantizer during reconstruction.

We will call our repeated measurement of $\tilde{x}$ that is subject to a certain error $\tilde{x^*}$. To perform reconstruction with $\tilde{x^*}$, we will first need to find all S quantizers for which we generated the helper data in the previous step.

We have to distinguish the two cases, that S is either even or odd:
If S is even, we need to define S quantizers offset by some distance φ. We can define the ideal position for the quantizer bounds based on its corresponding metric as centered around the center of the related metric.

We can find these new bounds graphically as depicted in Figure 11. We first determine the x-values of the centers of a metric (here M1, as shown with the arrows). We can then place the quantizer steps with step size Δ (Equation 7) evenly spaced around these points. With these new points for the vertical steps of $\mathcal{Q}$, we can draw the new quantizer for the first metric in Figure 12.

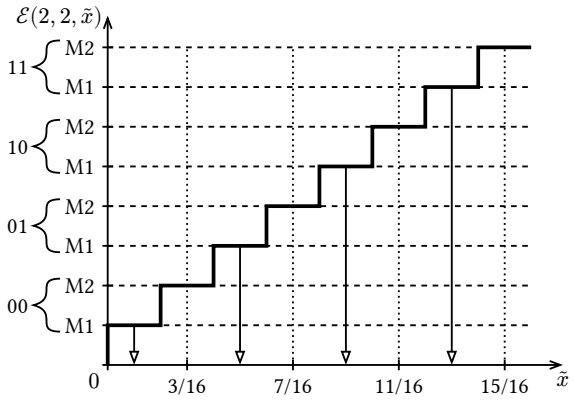

Figure 11: Ideal centers and bounds for the M1 quantizer

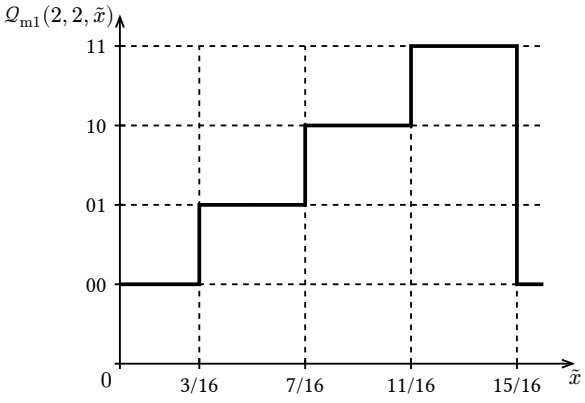

Figure 12: Quantizer for the first metric

As for metric 2, we can apply the same strategy and find the points for the vertical steps to be at $\frac{1}{16}$, $\frac{5}{16}$, $\frac{9}{16}$ and $\frac{13}{16}$. This quantizer is shown together with the first-metric quantizer in Figure 13, forming the complete quantizer for the reconstruction phase of a 2-bit 2-metric configuration $\mathcal{R}(2,2,\tilde{x})$.

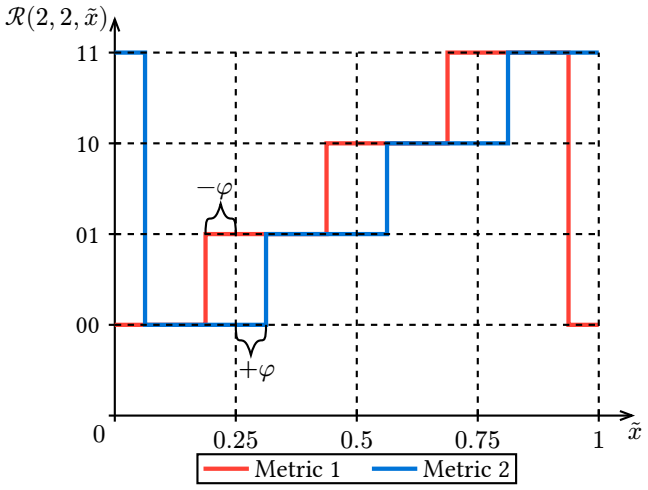

Figure 13: 2-bit 2-metric reconstruction quantizer

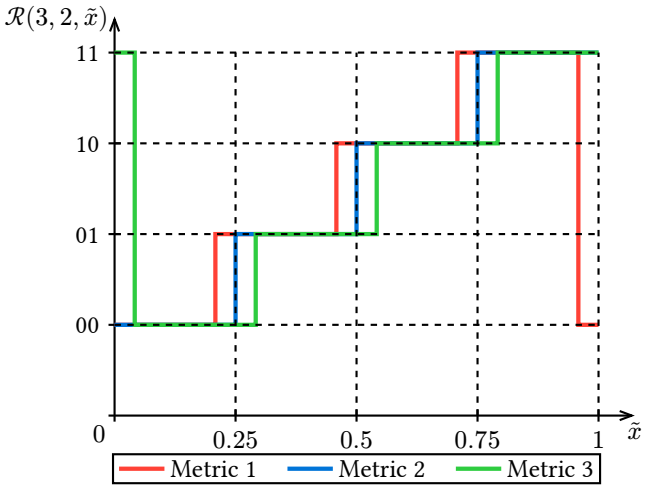

Figure 14: 2-bit 3-metric reconstruction quantizer

Analytically, the offset we are applying to $\mathcal{E}(2,2,\tilde{x})$ can be defined as

$$\Phi = \frac{1}{2^M \cdot S \cdot 2}\bigg|_{M=2,S=2} = \frac{1}{16} \quad . \tag{12}$$

Φ is the constant that we will multiply with a certain metric index i to obtain the metric offset φ, which is used to define each of the S different quantizers for reconstruction. In Figure 13, the two

metric indices $i = \pm 1$ will be multiplied with Φ, yielding two quantizers, one moved $\frac{1}{16}$ to the left and one moved $\frac{1}{16}$ to the right.

If a odd number of metrics is given, the offset can still be calculated using Equation 12. Additionally, we will keep the original quantizer used during enrollment as the quantizer for metric $\frac{s-1}{2}$ (Figure 14).

To find all metric offsets for values of $S > 3$, we can use Algorithm 1. For application, we calculate φ based on S and M using Equation 12. The resulting list of offsets is correctly ordered and can be mapped to the corresponding metrics in ascending order.

Algorithm 1: Find all offsets φ

```
input Φ, S
list offsets φ
if S is odd
    S = s − 1
    append 0 to list offsets
while i ≤ S/2
    append +(i · Φ) to list offsets
    append −(i · Φ) to list offsets
sort list offsets in ascending order
return offsets
end
```

Offset properties

Before we go on and experimentally test this realization of the S-Metric method, let's look deeper into the properties of the metric offset value φ.
Comparing Figure 13, Figure 14 and their respective values of Equation 12, we can observe, that the offset Φ gets smaller the more metrics we use.

Table 1: Offset values for 2-bit configurations

M	1	2	3	4	5	6	7	8	9	10
Φ	$\frac{1}{8}$	$\frac{1}{16}$	$\frac{1}{24}$	$\frac{1}{32}$	$\frac{1}{40}$	$\frac{1}{48}$	$\frac{1}{56}$	$\frac{1}{64}$	$\frac{1}{72}$	$\frac{1}{80}$

As previously stated, we will need to define S quantizers, $\frac{S}{2}$ times to the left and $\frac{S}{2}$ times to the right. For example, setting parameter S to 4 means we will need to move the enrollment quantizer $\frac{S}{2}\Big|_{S=4} = 2$ times to the left and right. As we can see in Table 2, φ for the maximum metric indices $i = \pm 2$ are identical to the offsets of a 2-bit 2-metric configuration. In fact, this property carries on for higher even numbers of metrics, as shown in Table 3.

Table 2: 2-bit 4-metric offsets

i	-2	-1	1	2
Metric	M1	M2	M3	M4
φ	$-\frac{1}{16}$	$-\frac{1}{32}$	$\frac{1}{32}$	$\frac{1}{16}$

Table 3: 2-bit 6-metric offsets

i	-3	-2	-1	1	2	3
Metric	M1	M2	M3	M4	M5	M6
φ	$-\frac{1}{16}$	$-\frac{1}{24}$	$-\frac{1}{48}$	$\frac{1}{48}$	$\frac{1}{24}$	$\frac{1}{16}$

At $s = 6$ metrics, the biggest metric offset we encounter is $\varphi = \frac{1}{16}$ at $i = \pm 3$.
This biggest (or maximum) offset is of particular interest to us, as it tells us how far we deviate from the original quantizer used during enrollment. The maximum offset for a 2-bit configuration φ is $\frac{1}{16}$ and we will introduce smaller offsets in between if we use a higher even number of metrics.

More formally, we can define the maximum metric offset for an even number of metrics as follows:

$$\varphi_{\text{max,even}} = \frac{\frac{S}{2}}{2^M \cdot S \cdot 2} = \frac{1}{2^M \cdot 4} \tag{13}$$

Here, we multiply Equation 12 by the maximum metric index $i_{\text{max}} = \frac{S}{2}$.

Now, if we want to find the maximum offset for a odd number of metrics, we need to modify Equation 13, more specifically its numerator. For that reason, we will decrease the parameter m by 1, that way we will still perform a division without remainder:

$$\varphi_{\text{max,odd}} = \frac{\frac{S-1}{2}}{2^n \cdot S \cdot 2} \tag{14.1}$$

$$= \frac{S-1}{2^M \cdot S \cdot 4}\bigg|_{M=2,S=3} = \frac{1}{24} \tag{14.2}$$

It is important to note, that $\varphi_{\text{max,odd}}$, unlike $\varphi_{\text{max,even}}$, is dependent on the parameter S as we can see in Table 4.

Table 4: 2-bit maximum offsets, odd

S	3	5	7	9
$\varphi_{\textbf{max,odd}}$	$\frac{1}{24}$	$\frac{1}{20}$	$\frac{3}{56}$	$\frac{1}{18}$

The higher S is chosen, the closer we approximate $\varphi_{\text{max,even}}$ as shown in Equation 15.1. This means, while also keeping the original quantizer during the reconstruction phase, the maximum offset for an odd number of metrics will always be smaller than for an even number.

$$\lim_{S\to\infty} \varphi_{\text{max,odd}} = \frac{S-1}{2^M \cdot S \cdot 4} \tag{15.1}$$

$$= \frac{1}{2^M \cdot 4} = \varphi_{\text{max,even}} \tag{15.2}$$

Because $\varphi_{\text{max,odd}}$ only approximates $\varphi_{\text{max,even}}$ if $S \to \infty$ we can assume, that configurations with an even number of metrics will always perform marginally better than configurations with odd numbers of metrics because the bigger maximum offset allows for better reconstructing capabilities.

2.3 Improvements

The by [1] proposed S-Metric Helper Data Method can be improved by using gray coded labels for the quantized symbols instead of naive ones.

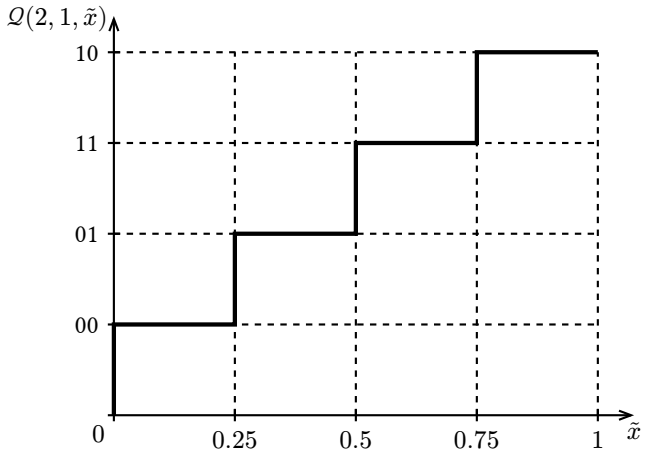

Figure 15: Gray Coded 2-bit quantizer

Figure 15 shows a 2-bit quantizer with gray-coded labelling. In this example, we have an advantage at $\tilde{x} = \sim 0.5$, because a quantization error only returns one wrong bit instead of two.

Furthermore, the transformation into the Tilde-Domain could also be performed using the eCDF to achieve a more precise uniform distribution because we do not have to estimate a standard deviation of the input values.

2.4 Experiments

We tested the implementation of Section 2.2 with the temperature dataset of [5]. The dataset contains counts of positives edges of a toggle flip flop at a set evaluation time D. Based on the count and the evaluation time, the frequency of a ring oscillator can be calculated using: $f = 2 \cdot \frac{k}{D}$. Because we want to analyze the performance of the S-Metric method over different temperatures, both during enrollment and reconstruction, we are limited to the second part of the experimental measurements of [5]. We will have measurements of 50 FPGA boards available with 1600 and 1696 ring oscillators each. To obtain the values to be processed, we subtract them in pairs, yielding 800 and 848 ring oscillator frequency differences *df*.
Since the frequencies *f* are normal distributed, the difference *df* can be assumed to be zero-mean Gaussian distributed. To apply the values *df* to our implementation of the S-Metric method, we will

first transform them into the Tilde-Domain using an inverse CDF, resulti/invite ng in uniform distributed values $\widetilde{df}$. Our resulting dataset consists of bit error rates (BERs) for quantization symbol widths of up to 6 bits evaluated with generated helper-data from up to 100 metrics. We chose not to perform simulations for bit widths higher than 6 bits, as we will see later that we have already reached a bit error rate of approx. 10% for these configurations.

2.4.1 Results & Discussion

The bit error rate of different S-Metric configurations for naive labelling can be seen in Figure 16. For this analysis, enrollment and reconstruction were both performed at room temperature and the quantizer was naively labelled.

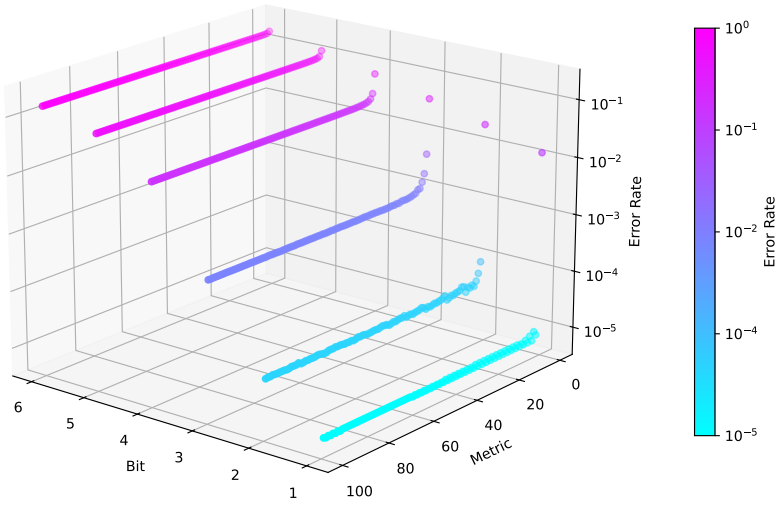

Figure 16: Bit error rates for same temperature execution. Here we can already observe the asymptotic loss of improvement in BERs for higher metric numbers

We can observe two key properties of the S-Metric method in Figure 16. The error rate in this plot is scaled logarithmically.
The exponential growth of the error rate of classic 1-metric configurations can be observed through the linear increase of the error rates. Also, as we expanded on in Section 2.2.2.1, using more metrics will, at some point, not further improve the bit error rate of the key. At a symbol width of $m \geq 6$ bits, no further improvement through the S-Metric method can be observed.

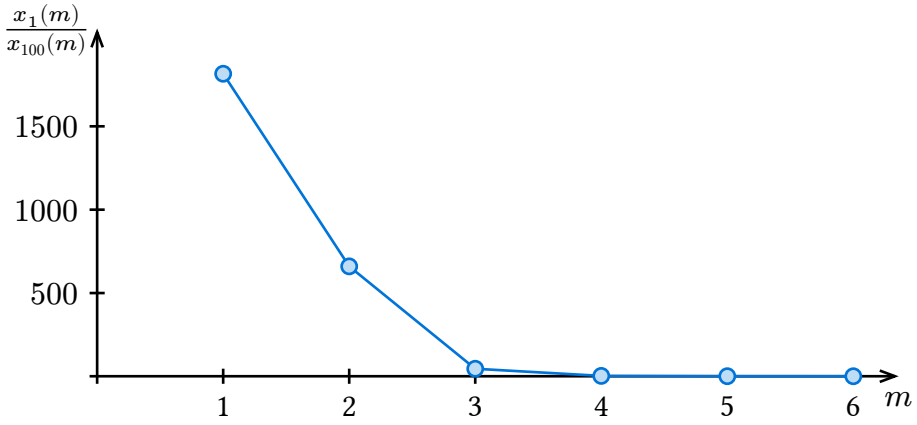

Figure 17: Asymptotic performance of SMHD

This tendency can also be shown through Figure 17. Here, we calculated the quotient of the bit error rate using one metric and 100 metrics. From $m \geq 6$ onwards, $\frac{x_1(m)}{x_{100}(m)}$ approaches ~1, which means, no real improvement is possible anymore through the S-Metric method.

2.4.2 Helper Data Volume Trade-off

2.4.3 Impact of temperature

We will now take a look at the impact on the error rates of changing the temperature both during the enrollment and the reconstruction phase.

The most common case to look at, is if we consider a fixed temperature during enrollment, most likely $25°C$. Since we wont always be able to recreate lab-like conditions during the reconstruction phase, it makes sense to look at the error rates at which reconstruction was performed at different temperatures.

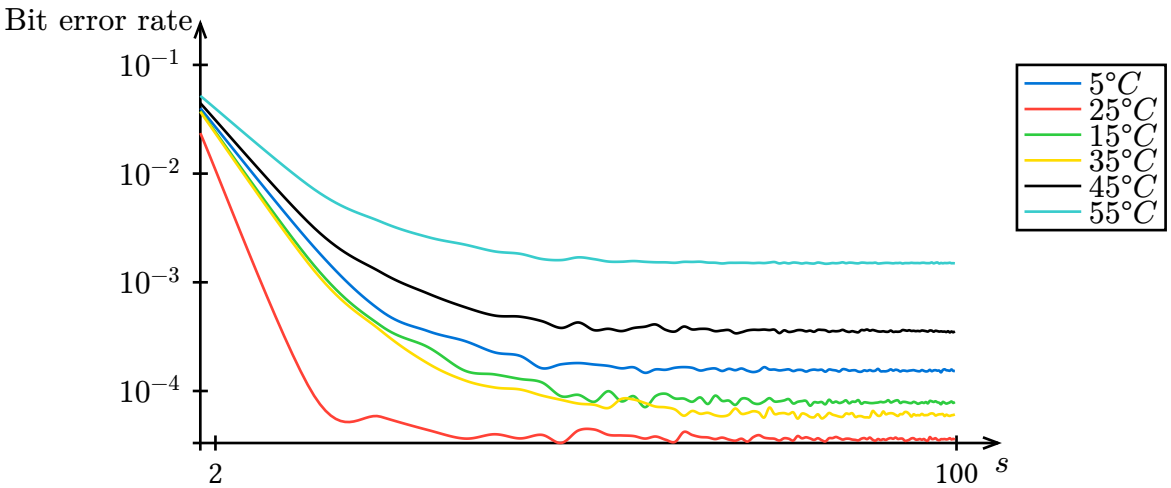

Figure 18: BERs for reconstruction at different temperatures. Generally, the further we move away from the enrollment temperature, the worse the BER gets.

Figure 18 shows the results of this experiment conducted with a 2-bit configuration.
As we can see, the further we move away from the temperature of enrollment, the higher the bit error rates turns out to be.

We can observe this property well in detail in Figure 19.

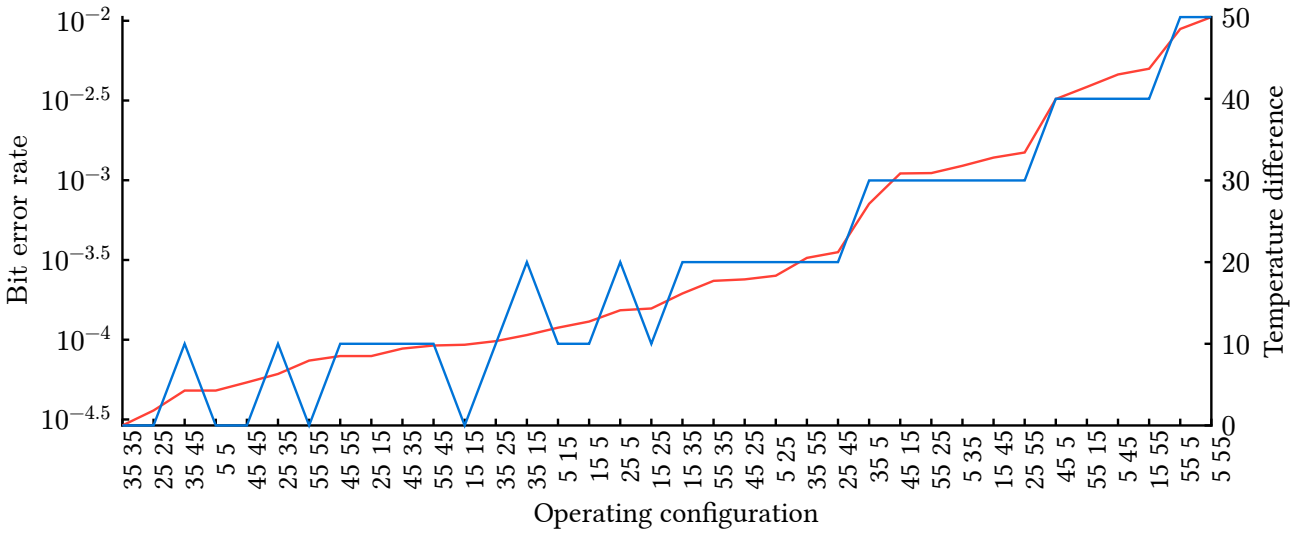

Figure 19: BERs for different enrollment and reconstruction temperatures. The lower number in the operating configuration is assigned to the enrollment phase, the upper one to the reconstruction phase. The correlation between the BER and the temperature is clearly visible here

Here, we compared the asymptotic performance of SMHD for different temperatures both during enrollment and reconstruction. First we can observe that the optimum temperature for the operation of SMHD in both phases for the dataset [5] is $35°C$ instead of the expected $25°C$. Furthermore, the BER seems to be almost directly correlated with the absolute temperature difference, especially at higher temperature differences, showing that the further apart the temperatures of the two phases are, the higher the BER.

2.4.4 Gray coding

In Section 2.3, we discussed how a gray coded labelling for the quantizer could improve the bit error rates of the S-Metric method.

Because we only change the labelling of the quantizing bins and do not make any changes to SMHD itself, we can assume that the effects of temperature on the quantization process are directly translated to the gray-coded case. Therefore, we will not perform this analysis again here.

Figure 20 shows the comparison of applying SMHD at room temperature for both naive and gray-coded labels. There we can already observe the improvement of using gray-coded labelling, but the impact of this change of labels can really be seen in Table 5. As we can see, the improvement rises rapidly to a peak at a bit width of M=3 and then falls again slightly. This effect can be explained with the exponential rise of the BER for higher bit widths M. For $M > 3$ the rise of the BER predominates the possible improvement by applying a gray-coded labelling.

Table 5: Improvement of using gray-coded instead of naive labelling, per bit width

M	1	2	3	4	5	6
Improvement	0%	24.75%	47.45%	46.97%	45.91%	37.73%

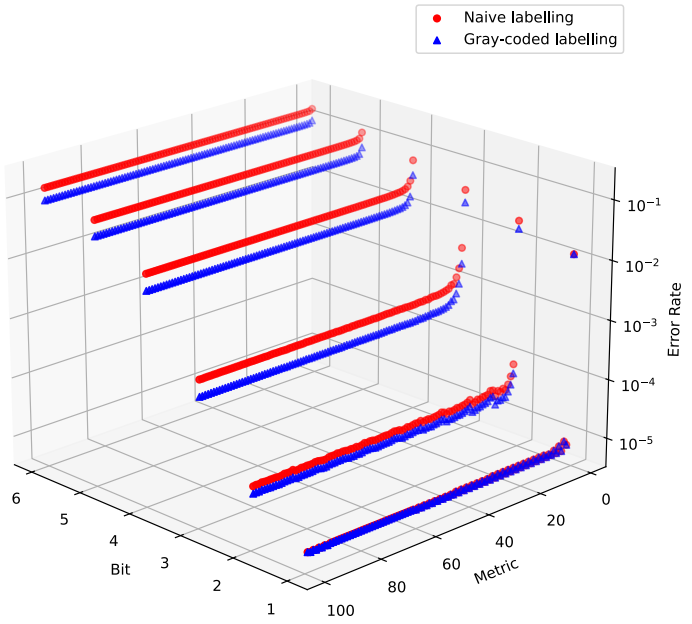

Figure 20: Comparison between BERs using naive labelling and gray-coded labelling

Using our dataset, we can estimate the average improvement for using gray-coded labelling to be at around 33%.

2.4.5 Usage of an eCDF

- eCDF kann die Gleichverteilung der quantisierten Symbole verbessern, da keine standardabweichung geschätzt werden muss, dafür komplexer zum ausrechnen
- Vergleich mit zwei histogrammen für die Gleichverteilung der Symbole?
- BER auswerten, ist wahrscheinlich schlechter

3 Boundary Adaptive Clustering with Helper Data

Instead of generating helper-data to improve the quantization process itself, like in SMHD, we can also try to find helper-data before performing enrollment that will optimize our input values before the quantization step to minimize the risk of bit and symbol errors during the reconstruction phase.

Since this HDA modifies the input values before the quantization takes place, we will consider the input values as zero-mean Gaussian distributed and not use a CDF to transform these values into the tilde-domain.

3.1 Optimizing a 1-bit sign-based quantization

Before we take a look at the higher order quantization cases, we will start with a very basic method of quantization: a quantizer, that only returns a symbol with a width of 1 bit and uses the sign of the input value to determine the resulting bit symbol.

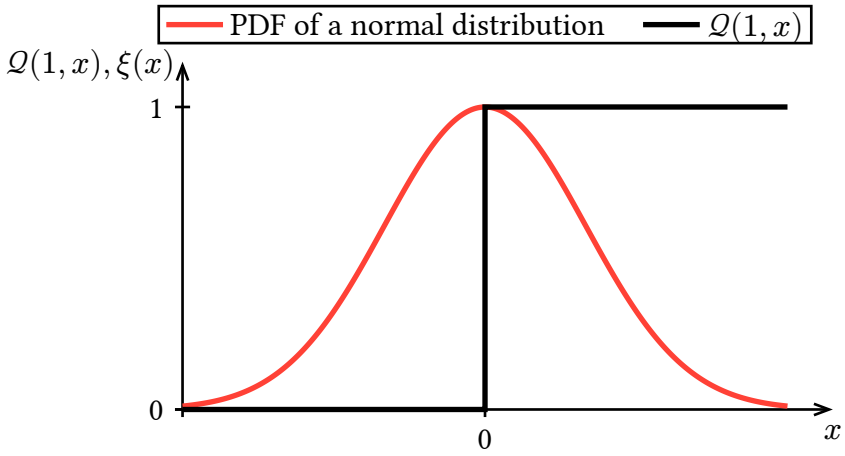

Figure 21: 1-bit quantizer with the PDF of a normal distribution

If we overlay the PDF of a zero-mean Gaussian distributed variable X with a sign-based quantizer function as shown in Figure 21, we can see that the expected value of the Gaussian distribution overlaps with the decision threshold of the sign-based quantizer. Considering that the margin of error of the value x is comparable with the one shown in Figure 2, we can conclude that values of X that reside near 0 are to be considered more unreliable than values that are further away from the x-value 0. This means that the quantizer used here is very unreliable without generated helper-data.

Now, to increase the reliability of this quantizer, we can try to move our input values further away from the value $x = 0$. To do so, we can define a new input value x^{lin} as a linear combination of two realizations of X, x_1 and x_2 with a set of weights h_1 and h_2:

$$x^{\text{lin}} = h_1 \cdot x_1 + h_2 \cdot x_2. \tag{16}$$

We can define the vector of all possible linear combinations $\boldsymbol{x}^{\text{lin}}$ as the vector-matrix multiplication of the two input values x_i and the matrix of all weight combinations:

$$\boldsymbol{x}^{\text{lin}} = \begin{pmatrix} x_1 \\ x_2 \end{pmatrix} \cdot \begin{bmatrix} h_1 & -h_1 & h_1 & -h_1 \\ h_2 & h_2 & -h_2 & -h_2 \end{bmatrix} \tag{17.1}$$

$$= \begin{pmatrix} x_1 \\ x_2 \end{pmatrix} \cdot \begin{bmatrix} +1 & -1 & +1 & -1 \\ +1 & +1 & -1 & -1 \end{bmatrix} \tag{17.2}$$

We will choose the optimal weights based on the highest absolute value of $\boldsymbol{x}^{\text{lin}}$, as that value will be the furthest away from 0. We may encounter two entries in $\boldsymbol{x}^{\text{lin}}$ that both have the same highest absolute value.

Lets take a look at the resulting random distribution of this process:

Glossary

***BER* – bit error rate**. 18, 19, 20, 21

***eCDF* – empirical Cumulative Distribution Function**. 5, 17, 21

***HDA* – helper data algorithm**. 9, 22

***SMHD* – S-Metric Helper Data Method**. 5, 10, 19, 20, 22

Bibliography

[1] R. F. Fischer, "Helper Data Schemes for Coded Modulation and Shaping in Physical Unclonable Functions," *arXiv preprint arXiv:2402.18980*, 2024.

[2] F. M. Dekking, *A Modern Introduction to Probability and Statistics: Understanding why and how*. Springer Science & Business Media, 2005.

[3] J.-L. Danger, S. Guilley, and A. Schaub, "Two-metric helper data for highly robust and secure delay PUFs," in *2019 IEEE 8th International Workshop on Advances in Sensors and Interfaces (IWASI)*, 2019, pp. 184–188.

[4] L. Tebelmann, U. Kühne, J.-L. Danger, and M. Pehl, "Analysis and protection of the two-metric helper data scheme," in *International Workshop on Constructive Side-Channel Analysis and Secure Design*, 2021, pp. 279–302.

[5] R. Hesselbarth, F. Wilde, C. Gu, and N. Hanley, "Large scale RO PUF analysis over slice type, evaluation time and temperature on 28nm Xilinx FPGAs," in *2018 IEEE International Symposium on Hardware Oriented Security and Trust (HOST)*, 2018, pp. 126–133.